Article

Not peer-reviewed version

Microfactory for Valorization of E-waste Plastics (Acrylonitrile-Butadiene-Styrene, Polycarbonate, and Polypropylene) on Additive Manufacturing Sector

Alejandro Moure Abelenda * and Farid Aiouache *

Posted Date: 30 March 2023

doi: 10.20944/preprints202303.0516.v1

Keywords: Melt-blend extrusion; 3D filament; brominated flame retardants; solvent extraction; acetone smoothing

Article

Microfactory for Valorization of E-Waste Plastics (Acrylonitrile-Butadiene-Styrene, Polycarbonate, and Polypropylene) on Additive Manufacturing Sector

Alejandro Moure Abelenda * and Farid Aiouache *

School of Engineering, Lancaster University, Lancaster, LA1 4YW; a.moureabelenda@lancaster.ac.uk

* Correspondence: a.moureabelenda@lancaster.ac.uk (A.M.A.); f.aiouache@lancaster.ac.uk (F.A.); Tel.: +44-7933712762 (A.M.A.); +44-1524593526 (F.A.)

Abstract: Less than half of e-waste plastics is sorted worldwide and this rate is likely to decline as major processing countries have banned importation of e-waste plastics. This forces the development of decentralized processing facilities, also known as microfactories. The present work investigates the recyclability of different grades of acrylonitrile-butadiene-styrene (ABS) copolymer, polycarbonate, and polypropylene, which were found to be very abundant in a recycling site in the UK. The determination of the matrix relied on the resin identification code imprinted in the e-waste plastic and subsequent FTIR analysis. The melt-blend extrusion technology enabled the valorization of the wasted thermoplastics as 3D filament without significant degradation of the polymers. The recycled materials maintained the tensile strength around 2.5 MPa in agreement with the specifications offered by virgin polymers. Further characterization was done by means of laser microscope, thermogravimetric analysis, and XRF to determine the commercial viability of the recycled filament. A modified solvent-based method was developed with acetone to remove the brominated flame retardants: 25g/100mL, 30 minutes of contact time, and 4 extraction steps. The FTIR results show that the degradation of the rubbery dispersed phase corresponding to the butadiene can be accumulated in the less soluble fraction of the waste ABS.

Keywords: melt-blend extrusion; 3D filament; brominated flame retardants; solvent extraction; acetone smoothing

1. Introduction

The fate of e-wastes is a growing concern of approximately 54 million tonnes per annum worldwide [1], which is estimated to double by 2050 [2]. The valorization of these materials is worth $64 billion but less than half of e-waste plastics are recycled globally [3,4]. The Basel Convention on the control of transboundary movements of hazardous wastes limits the cooperation between countries to handle e-waste [5].Furthermore, the rate is likely to decline as major processing countries are progressively banning importation of plastic wastes [6]. Therefore, since the modest global recycling efforts underway are crushed, there is a need for decentralized and highly specialized plastic recycling sites (also known as microfactories) that also reduce the transport costs [4,7]. E-waste plastics occupy large space on the premises of the recycling companies and the process of identification and sorting is challenging owing to the wide range of polymer mixtures that are used to get the desired properties [8]. The primary or secondary recycling capabilities using mechanical separation by reading the Resin Identification Code (RIC), which is indented in the e-waste plastics [8,9], avoids the loss of functionalities of the polymers, hence these technologies are preferred to other types of upgradation methods. In this way the recycled materials can be used for the same or similar purposes as the original product [4]. Although tertiary and quaternary recyclings are less cost-effective, these technologies are applied to deal with complex mixtures of polymers, when the mechanical separation is not sufficient [10]. However, a combination of these technologies (i.e. tertiary chemical treatment with quaternary energy production) can be used to improve techno-economically the performance of the downstream process. For example, removal of brominated

 doi:10.20944/preprints202303.0516.v1

flame retardants (BFR) by solvent extraction to enhance the thermal decomposition and mass loss in a subsequent pyrolysis step [10,11]. It should be noted that some type of BFR can be in concentrations up to 30% by weight, which means that 1 kg of polymer would contain 50 – 300 g of flame retardant [12]. On the other hand, the solvent extraction of the BFR might not be convenient for optimizing the downstream processing of primary or secondary mechanically separated polymers. For example, in the manufacturing of different plastic components of the casing of electrical devices the melt-blend extrusion is carried out at temperatures at slightly greater than the melting point. Since the effect of flame retardants can be noticeable even at temperature closed to the glass transition, the presence of these additives might avoid the mass loss of the polymer that is being extruded and, importantly, the emission of pollutants of the ABS [13].

With these notions in mind, the design of a microfactory for recycling e-waste plastics primarily composed of acrylonitrile-butadiene-styrene copolymer (ABS), polycarbonate (PC), and polypropylene (PP) was investigated in the present article, because they were found to be very abundant in a recycling site in the UK. The ABS and the PC are the main components in telephone handsets, keyboards, monitors, and computer housing, while the PP is widely employed for the manufacturing of boxes and casings. The research objectives were: (a) to find out synergistic approaches of combining these materials, (b) to define the specifications of the equipment required for the processing, and (c) to identify the best component that can be replicated as the best route for the valorization of the e-waste plastic. Given the open-source license of recyclebots and their versatility [9,14], this type of equipment was considered suitable for the design of a valorization process and the scaleup to modest real conditions of the rate of handling e-waste plastics by medium-size recycling enterprises (~300 tonnes per annum). In this way, following the instructions of the manufacturer of the melt-blend extruder [15–18], virgin polymers were employed to initiate the melt-blend extrusion process and the share of the fresh materials was progressively decreased until the point of operating the equipment with 100 % e-waste plastic. Unlike the selection of the grades of the virgin material, which was based on its Melt-Flow Index (MFI), the different grades of the waste ABS were identified by the flow regime in the extruder and the color of the waste ABS (i.e. white or black). The valorization of the thermoplastics as 3D filaments for additive manufacturing was subsequently confirmed by printing a specimen, in agreement with the methodology of Arostegui et al. [19], to increase the technology readiness level.

2. Results

The following subsections include the data that support the design of a microfactory for processing ABS, ABS+PC, and PP.

2.1. Collection of the waste and shredding

The bulkiest e-waste plastics were identified in a recycling company (Figure 1a) and subsequently shredded to less than 5mm (Figure 1b). As can be appreciated in Figure 1, the sample of ABS+PC was more heterogenous than the other samples: white ABS, black ABS, and PP. Thereby, it can be expected a low adhesion of the particles of ABS+PC during the extrusion process and the need of using a compatibilizer or impact modifier to improve the tension strength of the 3D filament produced with this e-waste plastic [20]. According to Ramesh et al. [21], the PC offers greater mechanical performance and is less susceptible to degradation than the ABS. On the other hand, the ABS is more fluid and its shear thinning behaviour is a major reason for improving processability of PC material. The compatibility or miscibility of the PC and ABS depends on the grade of the ABS and the content of the acrylonitrile monomer [21].

Preprints (www.preprints.org) | NOT PEER-REVIEWED | Posted: 30 March 2023 doi:10.20944/preprints202303.0516.v1

(a) **(b)**

Figure 1. Bulkiest e-waste plastics identified in the recycling company: **(a)** raw samples and **(b)** shredded sample to a particle size to less than 5 mm: white ABS (top-left corner), black ABS (top-right corner), ABS+PC (bottom-left corner), and PP (bottom-right corner).

2.2. Characterization of the matrix and the additives of the e-waste plastics

In addition to the RIC, the difference between the matrices of the e-waste plastics was confirmed with Fourier-transform infrared spectroscopy (FTIR) and X-ray fluorescence (XRF) analysis (Figure 2). Figure 2 shows the FTIR profile of the e-waste plastics (white ABS, black ABS, ABS+PC, and PP), the virgin polymers employed to assist the melt-blend extrusion (ABS, high-density polyethylene (HDPE), and polylactic acid (PLA)), and the purge material recommended for the cleaning of the equipment after the operation (i.e., Devoclean MidTemp purge). The most characteristic peak that was identified for the ABS was found at the 2,200 cm^{-1}, corresponding to the nitrile group [19]. The larger error band found for the ABS+PC in Figure 2a is associated with the greater variability of the matrix of this heterogeneous sample. With regard to the initial characterization of the samples in terms of XRF (Figure 2b): calcium, sulfur, and phosphorus were found to be the trace elements most abundant in all the samples, but it is also important to highlight the presence of BFR in the sample of white ABS.

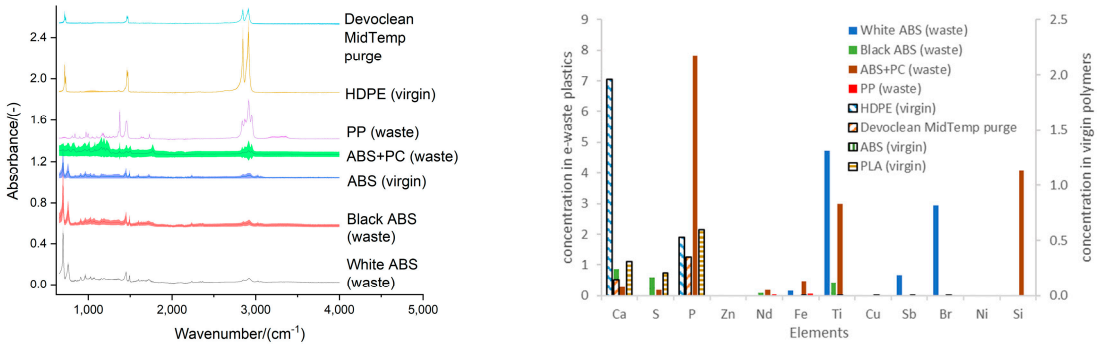

(a) **(b)**

Figure 2. Characterization of the composition of the e-waste plastics (ABS, PC, and PP) and the virgin polymers used to enable the melt-blend extrusion process for the production of 3D filament: (**a**) matrix in terms of FTIR spectra; (**b**) additives as described by the XFR results.

2.3. Melt-blend extrusion

The melt-blend extrusion process was performed following the advice provided by the manufacturer of the compounder: starting with virgin materials and progressively increase the share of waste. This can be seen in Figure 3a for the white ABS. It was necessary to use the HDPE and the PLA as transition polymers for the ABS and the PP, respectively, in order to obtain the 3D filament with 100 % recycled material (Figure 3b).

Preprints (www.preprints.org) | NOT PEER-REVIEWED | Posted: 30 March 2023 doi:10.20944/preprints202303.0516.v1

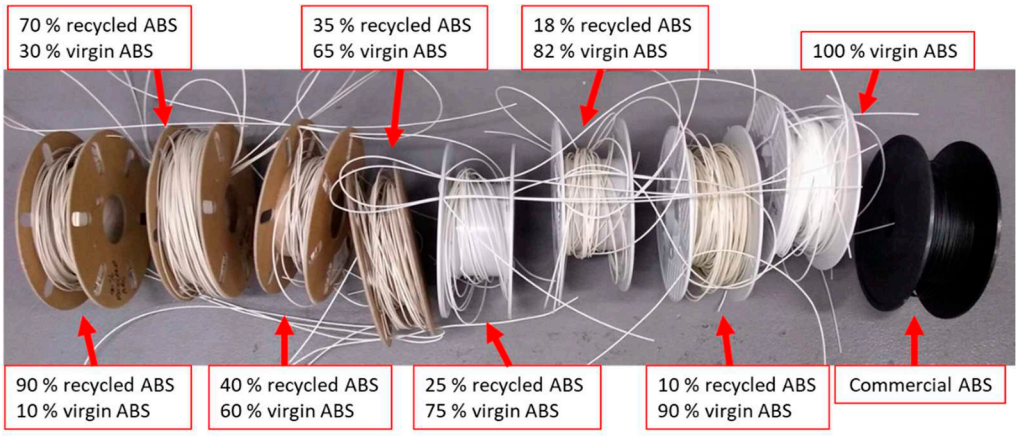

(**a**)

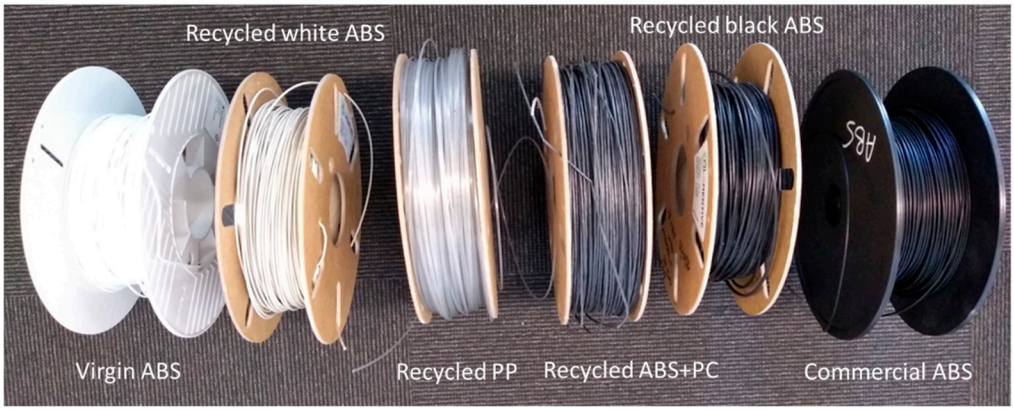

(**b**)

Figure 3. (a) Progressive increase in the share in the share of e-waste plastic (white ABS) and decrease in that of the virgin polymer (ABS). **(b)** 3D filament prepared with 100 % recycled material: white ABS, black ABS, PP, and ABS+PP.

2.4. 3D filament diameter

The filament thickness monitored with the optical sensor of the 3devo compounder during the recycling of the waste ABS, PC, and PP is show in Figure 2. Additionally, the quality check was performed with PLA, following the recommendation of the manufacturer of the recyclebot [22], to confirm that the equipment was operating properly and the fluctuation observed were derived by the processing of the complex waste material. The white ABS was found to be the most suitable material to be valorized as 3D filament via melt-blend extrusion, as it was easier to get the filament diameter in the range of 1.75 ± 0.10 mm (< 8,000 s in Figure 2a). The black ABS was more susceptible to clog the recyclebot and it was necessary (> 8,000 s in Figure 2a) to repeat the preparation of the 3D filament for this matter (> 15,000 s in Figure 2b). Similarly, the recycling with the ABS+PC (< 15,000 s in Figure 2b) and PP (Figure 2c) was challenging, with difficulties maintaining a constant diameter of the 3D filament. The quality check with PLA (Figure 2d) informed on the difficulty of continuously measuring the filament thickness with the waste polymers: with these recycled materials, the diameter thickness went to zero multiple times during the operation of the compounder because the filament is dancing and going out of the optical sensor.

Preprints (www.preprints.org) | NOT PEER-REVIEWED | Posted: 30 March 2023 doi:10.20944/preprints202303.0516.v1

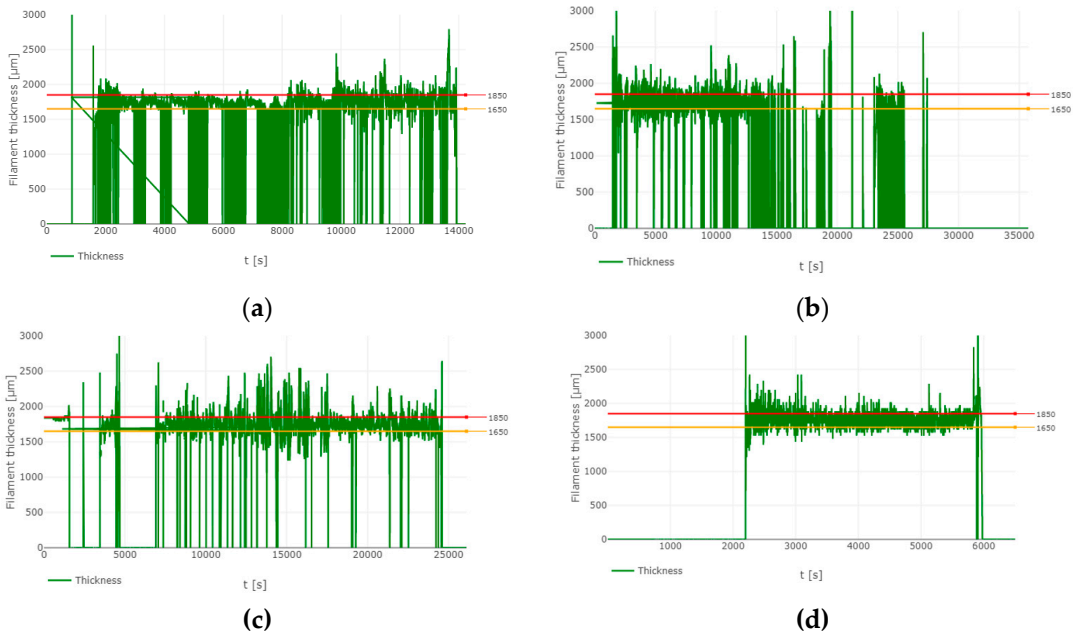

Figure 4. Filament diameter obtained via melt-blend-extrusion of the different e-waste plastics: (**a**) white ABS (initial 2 hours) and black ABS (remaining 2 hours); (**b**) ABS+PC (initial 4 hours) and black ABS (remaining 4 hours); (c) PP; (d) quality check with PLA.

2.5. 3D printing

The feasibility of the 3D printing with the recycled filament was tested (Figure 5a) to prepare a dumbbell-shaped specimens (Figure 5b), according to the British Standard EN ISO 527-2:2012 (test conditions for molding and extrusion), and to characterize the performance of the recycled material in the mechanical testing. A limited number of dog-bone specimens could be prepared due to presence of lumps in the filament that clogged the 3D printer (Figure 5c). This was associated with the poor shredding of the samples (presence of 2-cm particles) and the unmelted particles leading to lumps of a diameter much greater than 1.75 mm, which were also consequence of the very short screw of the melt-blend-extruder that did not promote the complete mixing of the samples of e-waste.

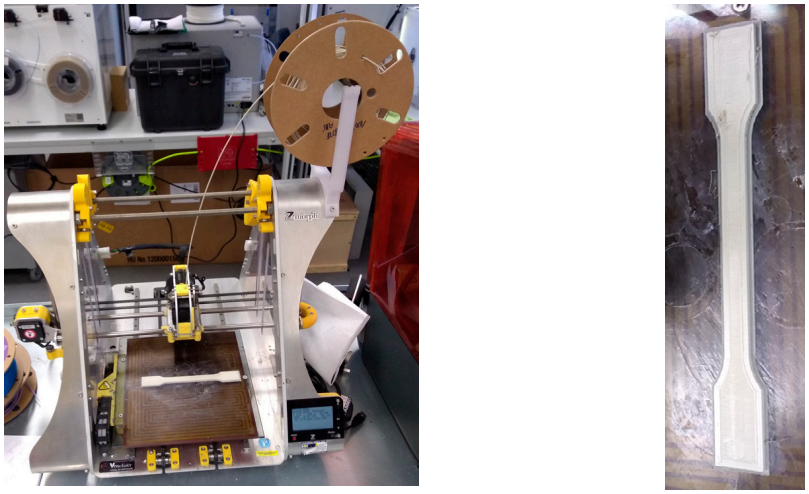

Preprints (www.preprints.org) | NOT PEER-REVIEWED | Posted: 30 March 2023 doi:10.20944/preprints202303.0516.v1

(c) **(d)**

Figure 5. (a) 3D printing of the dumbbell shaped specimen for tensile testing; **(b)** dumbbell shaped specimen (zoom in); **(c)** 1.75±0.20-diameter lumps in the 3D filament (100 % white ABS); and **(d)** 2-cm particles in shredded white ABS.

2.6. Tensile testing

The recycled materials have an average tensile strength around 2.5 MPa and the greatest tensile strength was found for the black ABS (4.14 ± 0.34 MPa) while the lowest correspond to the ABS+PC (1.70 ±0.36 MPa). The blend of the waste materials with the virgin polymers did not offer a greater tensile strength, compared to the 3D filament produced with 100 % recycled material. It is important to highlight that the tensile strength reported in Figure 6a refers to the maximum force than the material can hold before staring the neck formation. Figure S1 shows the neck formation in the PP. It is noteworthy to mention that for the calculation of the tensile strength, a homogeneous diameter of 1.75 mm was assumed for all filaments. This implied that the cross-sectional area considered for the filament (2.41 mm^2) was approximately 10 times smaller than that for the dumbbell-shaped specimen (40 mm^2; [23]). Nevertheless, the tension strength measure for the dog-bone specimen of white ABS (1.54 MPa) was in the same order of magnitude because the maximum force reached was also approximately 10 times greater (0.0617 kN; Figure S2) than what was achieved with the filament of white ABS (Figure 6b). These results were an order of magnitude lower than those reported by Zhang et al. [24], who used virgin HDPE to support the recycling of the waste HDPE. In the present study, the HDPE did not enhance the tensile strength of the ABS filament as there was a weak interaction between these polymers. This can be seen in the lose threads upon rupture of the filaments of HDPE and ABS in the tensile testing (Figure S3). Figure 6c, Figure 6d, and Figure 6e show the profiles of the tensile force versus the displacement for the black ABS, ABS+PC, and PP. The profiles tensile force versus extension of the remaining combination of polymers are shown in Figures S4–S7.

Preprints (www.preprints.org) | NOT PEER-REVIEWED | Posted: 30 March 2023 doi:10.20944/preprints202303.0516.v1

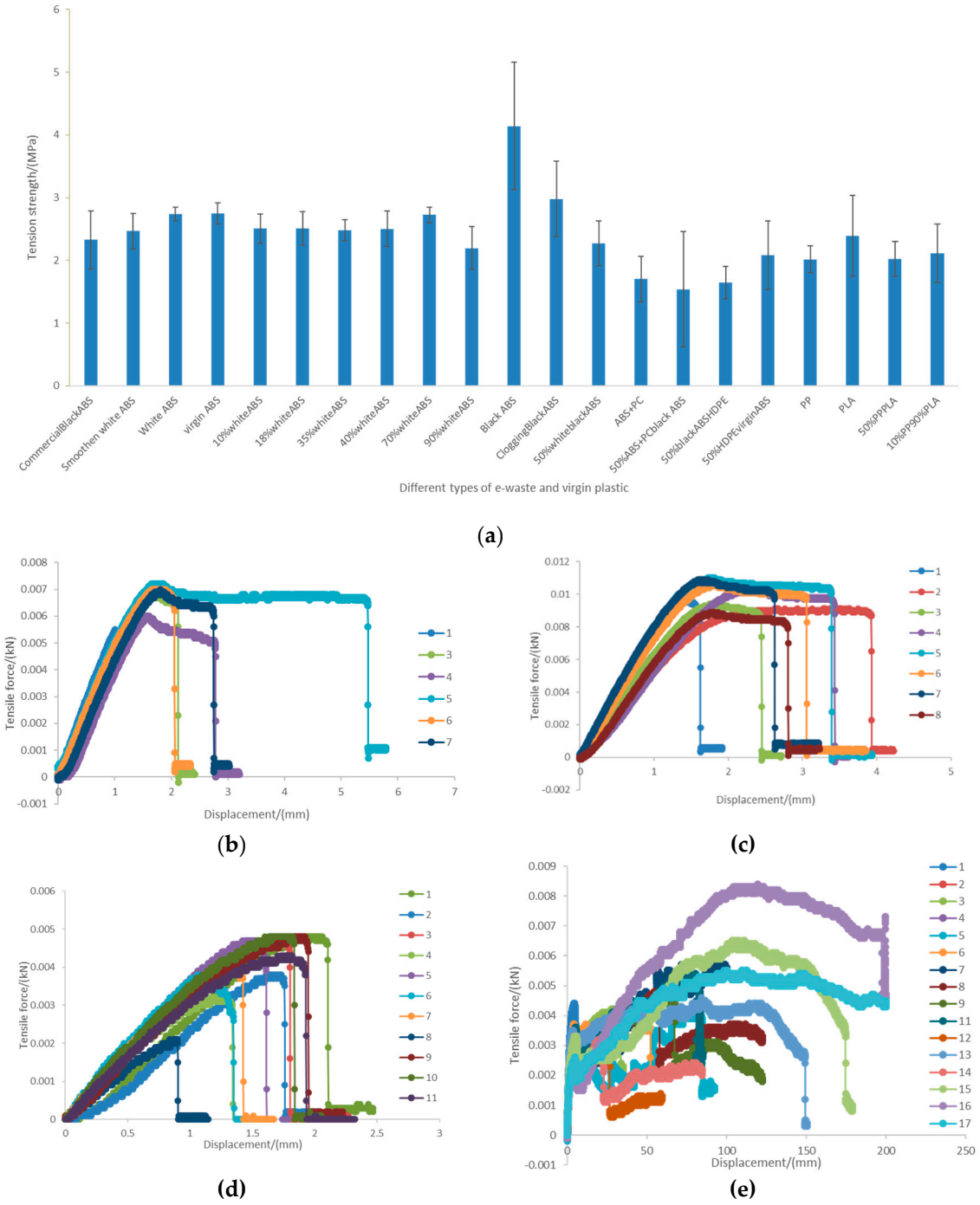

Figure 6. (**a**) summary of the mechanical strength of the 3D filament; (**b**) profile tensile force vs extension of the 7 replicates of the white ABS filament; (**c**) profile tensile force vs extension of the 8 replicates of the black ABS filament; (**d**) profile tensile force vs extension 11 replicates of the ABS+PC filament; and (**e**) profile tensile force vs extension of the 17 replicates of the PP filament.

According to the empirical results, the neck formation can be seen with less than 2 mm of elongation of the filament. In the case of the white and black ABS, the elongation before failure was not found beyond 6 mm (Figure 6b,c). As the filament of ABS+PC is brittle due to the heterogeneity nature of the sample (Figure 1), there is no neck formation and minimum elongation took place before the breakage of the specimens (Figure 6d). The maximum displacement that was allowed for the tensile testing was 200 mm but this was not enough for the PP, as this material was found to be very flexible without breaking even at 200 mm of deformation (Figure 6e). The melt-blend extrusion process did not affect negatively the degradability of the e-waste plastics, as several changes in the

 doi:10.20944/preprints202303.0516.v1

conformation of the matrix polymers could be identified in the raw samples and in the recycled filaments: including the glass transition temperature, crystallization temperature and melting point (Figures S8–S12). Although similar weight loses were found in the samples of plastic before and after the melt-blend extrusion, in general (except for the black ABS; Figure S9) it could be considered that the extruded samples are more recalcitrant as the number of endothermic degradation reactions increased [25], particularly at high temperatures (above 400 ºC). As can be seen in Figure S13, conducting the coupled thermogravimetric analysis (TGA) and differential scanning calorimetry (DSC) at temperature up to 800 ºC affected the behavior of the recycled white ABS filament and the commercial black ABS, increasing in both cases the proliferation of endothermic reactions both at the beginning and towards the end of the analysis.

The impact of the storage conditions on the behavior of the polymers was also assessed with the TGA/DSC. The storage of the HDPE at room conditions makes this material more recalcitrant and hinders its processability with the melt-blend extrusion (Figure S14). The other material that the manufacturer of the compounder allows to be left in the shutdown equipment is the PLA and its comparison with the HDPE is also show in Figure S14. Figure S14 confirmed that the Devoclean MidTemp purge recommended by the manufacturer was also polyethylene. The similarities between the HDPE and the Devoclean MidTemp purge can be seen in the comparison of the FTIR spectra offered in Figures 2 and S15.

2.7. Aesthetic properties

The performance of the recycled filament was also characterized with the laser microscope using 5 times (x5), 10 times (x10), and 20 times (x20) magnifications. This equipment was used to create a 3D model of the specimens, which were prepared with the blends of polymers: the color scales in Figure 7 and the supplementary materials represent the depth of the laser microscope images. In the broken dumbbell-shaped specimen (Figure 7a), many fibers can be appreciated due to the way this component is manufactured with the 3D printer (Figure 7b). It is expected that if the dog-bone was prepared via molding injection, a cleaner rupture would be obtained. In fact, the rupture of filaments made with white ABS (Figure 7c) and the black ABS (Figure 7d) was clean with minimum neck formation. The same behavior was observed for a commercial filament of black ABS (Figure S16). However, when the black ABS and the white ABS were combined the resulting filament was more flexible and allowed the neck formation (Figure S17). Figure S17 shows the failure of the filament prepared with a blend of 50 % white ABS and 50 % black ABS. The supplementary material contains more laser microscope images of the filaments of a progressive increase in the share of white ABS, in relation to virgin ABS, at the point of rupture (Figures S18–S21,S23,S25,S27) and their neck formation (Figures S22,S24,S26). Figure S28 shows the failure of the filament prepared with virgin ABS. Figure S29 shows the rupture of the filament prepared with a blend of 50 % HDPE and 50 % black ABS. Figure S30 shows the neck formation in the filament prepared with a blend of 50 % HDPE and 50 % black ABS. Although the combination of black ABS with HDPE provided similar results to that of ABS+PC, in terms of tensile strength (Figure 6a), the aesthetic behavior upon failure was different. Figure S29 and Figure S30 justify that the interaction of between the black ABS and the HDPE was greater than the compatibility of the ABS+PC (Figure 7e). As can be seen in Figure 7e, the tenacity of the ABS+PC was lower than that of the black ABS+HDPE because the former did not have significant neck formation before the rupture. The brittleness of the filament ABS+PC can also be appreciated on the many fibers that can be seen in the broken specimens (Figure 7e). A closer look to the striations of the ABS+PC can be seen in Figure S31. The greatest flexibility was obtained with the filaments of PP; thus, its behavior was mainly characterized by the reduction of the cross-sectional area to enable the extension and ovoid the failure under a traction force (Figure 7f). Additionally, Figure S32 displays a filament of PP that showed fibrous behavior upon rupture in the tensile testing. It is important to clarify that the filament of PP was transparent and the black part in the microscope pictures was the color of the base of the sample holder (Figure 7f). In Figure 7f the white part of the filament resulted from stretching and neck formation. Even the addition of PLA in shares of 50 % (Figure S33) and 90 % (Figures S34 and S35) did not reduce the transmittance of the material. The

Preprints (www.preprints.org) | NOT PEER-REVIEWED | Posted: 30 March 2023 doi:10.20944/preprints202303.0516.v1

ratio of PLA to PP however affected the fibrous behavior, as more fibers were observed when both materials were combined at approximately the same rate because this enhanced the incompatibility between the 2 polymer types (Figure S33). These fibers were not originally present in the filament of PLA (Figures S36 and S37).

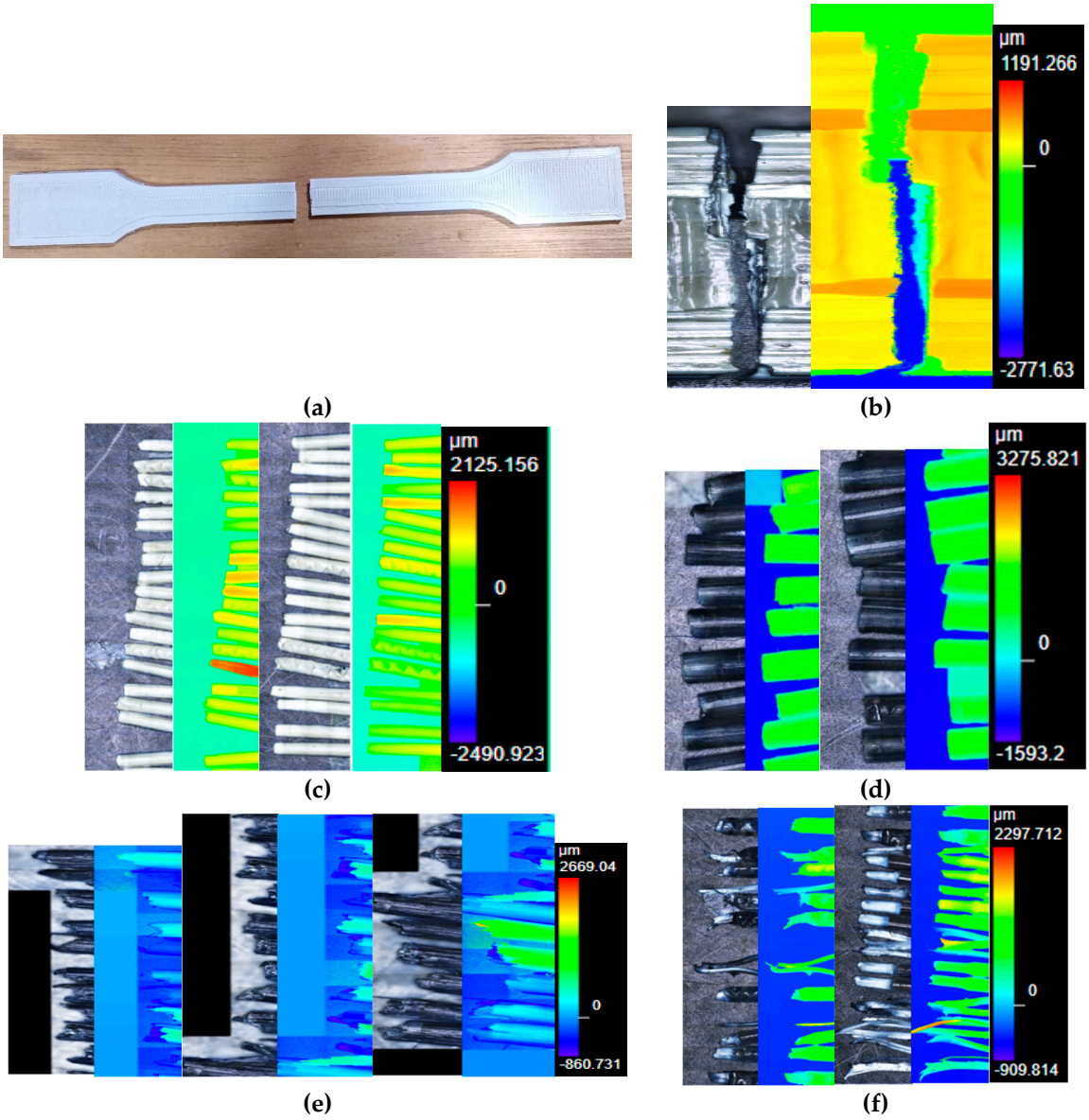

Figure 7. (a) dumbbell shaped specimen after the tensile testing; **(b)** laser microscope image (x5) of the dumbbell shaped specimen at the point of failure; **(c)** laser microscope image (x5) of the white ABS filaments at the point of rupture; **(d)** laser microscope image (x5) of the black ABS filaments at the point of failure; **(e)** laser microscope image (x5) of the black ABS filaments at the point of rupture; **(f)** laser microscope image (x5) of the ABS+PC filaments at the point of failure; and **(g)** laser microscope image (x5) of the PP filaments at the point of rupture.

2.8. Acetone-based treatment of the ABS

The acetone smoothing is widely applied to polish the pieces of ABS prepared by additive manufacturing. This is because the ABS is soluble in acetone and the 3D printed parts have marks (Figure 7a,b) that need to be removed before reaching the final customer, in case the product will be seen. For the sake of designing the valorization process of the e-waste plastic, the effect of the acetone treatment was analyzed at 2 levels: properties of the matrix of ABS and concentration of trace elements. Additionally, the treatments of the e-waste plastics with dichloromethane (DCM) and nitric acid were also evaluated.

Preprints (www.preprints.org) | NOT PEER-REVIEWED | Posted: 30 March 2023 doi:10.20944/preprints202303.0516.v1

2.8.1. Impact in the properties of the matrix

The chemical refining of the ABS with acetone could hinder the recyclability of this polymer, due to the degradation of the less soluble fraction of rubbery dispersed phase of butadiene. The possible changes in the chemical structure of the extracted e-waste plastics were studied by FTIR (Figures 8–10). The serial extractions (up to 4 times) were performed by mixing of 25 g of each e-waste plastic with 100 mL of acetone (fresh solvent added in each extraction step) for 30 minutes. The fraction of ABS extracted with the acetone was subdivided in the supernatant (most soluble components of the ABS) and the pellet. Additionally, the remaining residue after the serial extractions was similarly divided into supernatant and pellet. The most characteristic absorbance band of the ABS at approximately 2,200 cm^{-1} (corresponding to the C≡N triple bond) could be seen in almost all the fractions of the e-waste plastics treated with acetone, with the exception of the ABS+PC (Figure 10) due to the lower concentration of the poly(styrene-acrylonitrile) (SAN) copolymer. In agreement with the findings of Arostegui et al. [19], the degradation of ABS with the serial extraction procedure upon these experimental conditions occurred in the pellet (i.e. butadiene-rich phase) and not in the more soluble SAN copolymer that mainly remained in the supernatant. In this way, the height of absorbance bands associated with the butadiene double bonds (910 cm^{-1} and 966 cm^{-1}) significantly increased in the pellet-fraction. Furthermore, the absorbance band related to saturated carbonyl groups (1,734 cm^{-1}) was progressively built up, particularly in the pellet of the 3rd extraction of the black ABS (Figure 9). According to Kim and Kang [26], the enhancement of these absorbance bands was due to the degradation of the butadiene phase, especially in unsaturated bonds, leading to the formation of carbonyl groups. Additionally, the N-H stretching (3,300 cm^{-1}) can be identified in the pellet of the 3rd extraction of the black ABS, indicating that the butadiene also reacts with the acrylonitrile. Only 3 extraction steps were considered for the black ABS (Figure 9) because this type of e-waste plastic appeared to be more soluble in acetone than the white ABS. In the case of ABS+PC (Figure 10), the residue that remained after the 4 acetone-extractions was not analyzed because this SAN-depleted material was further treated with DCM for the extraction of the PC [27].

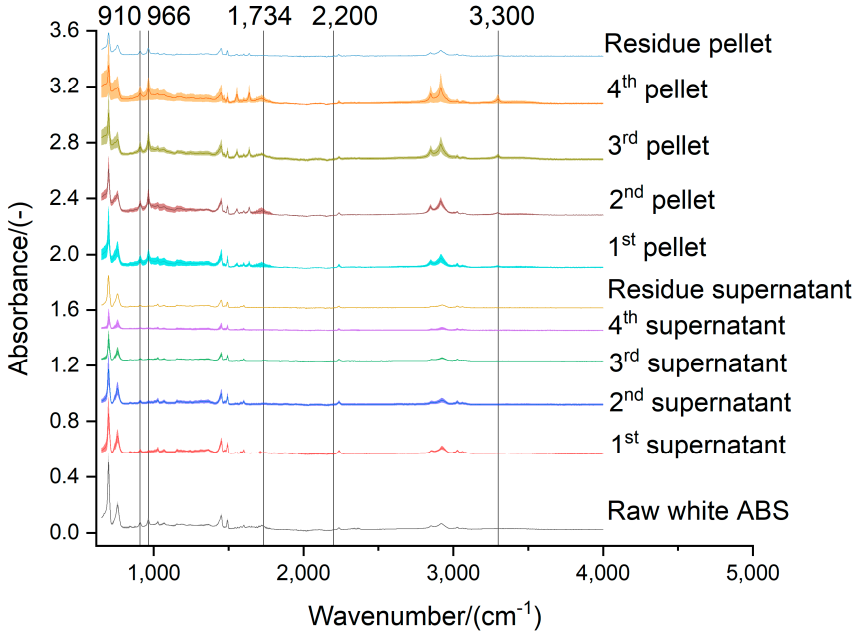

Figure 8. Effect of the acetone extraction on the functional groups of the white ABS

Preprints (www.preprints.org) | NOT PEER-REVIEWED | Posted: 30 March 2023 doi:10.20944/preprints202303.0516.v1

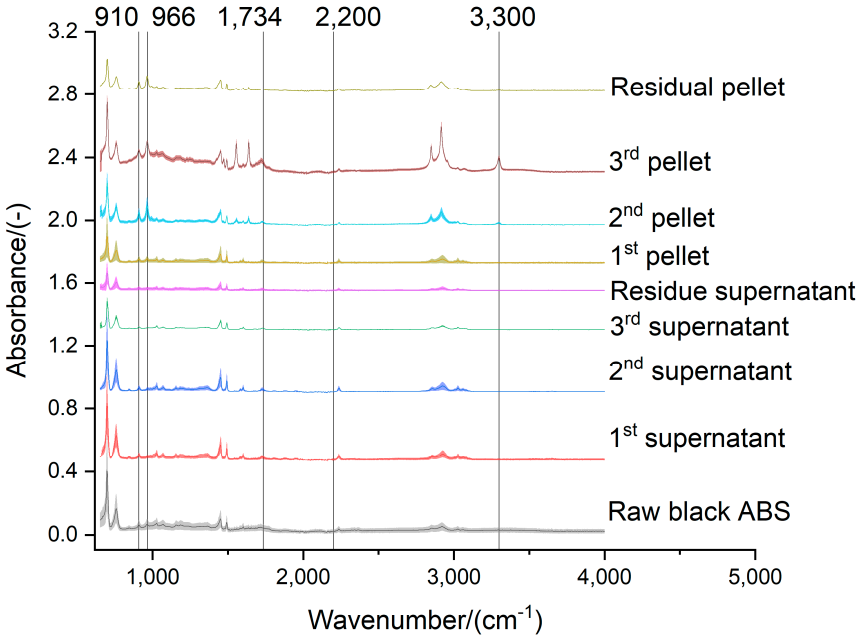

Figure 9. Effect of the acetone extraction on the functional groups of the black ABS

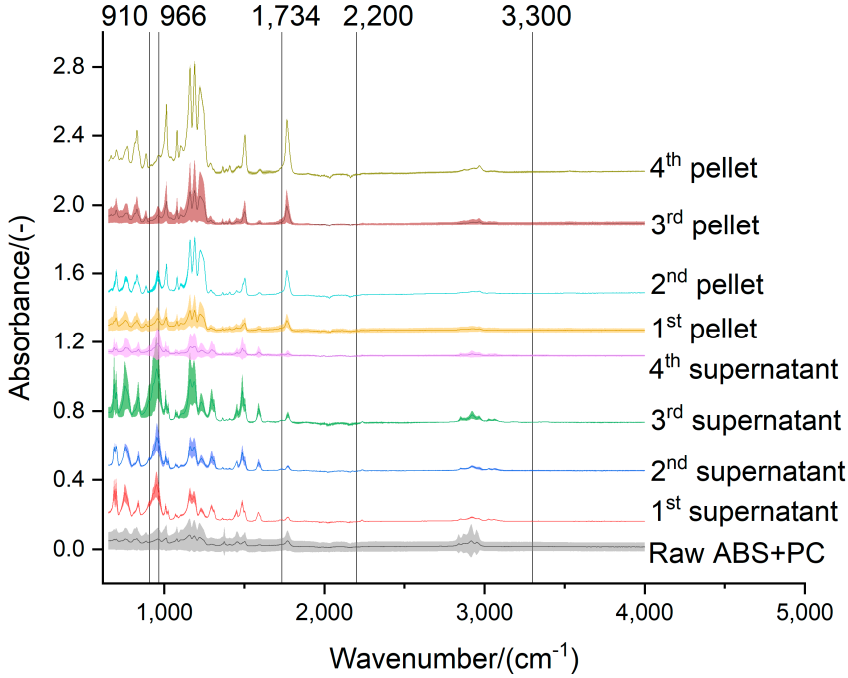

Figure 10. Effect of the acetone extraction on the functional groups of the ABS+PP.

In addition to the interpretations based on the FTIR profiles of the acetone treated e-waste plastics, the TGA/DSC (Figures S38–S44) were also considered for the design of a more advantageous extraction step. The white ABS lost its functionality beyond the 2nd extraction, as this can be seen in the smoother DSC curves in Figures S38 and S39. A single treatment with the nitric acid disabled any possible phase change in the white ABS (Figure S40). For the acetone-treatment of black ABS, 2 extraction steps were also found to be the optimum, since beyond that point the phase changes are minimized (Figures S41 and S42). Finally, for the valorization of the ABS+PC, it might not convenient to conduct the 4th extraction step with acetone, as the DSC profiles (Figures S43 and S44) show a change in the trends of phase change at that point, particularly with the predominance of exothermic reactions at lower temperatures indicating easier degradation of the polymer.

Preprints (www.preprints.org) | NOT PEER-REVIEWED | Posted: 30 March 2023 doi:10.20944/preprints202303.0516.v1

2.8.2. Change in the composition of trace elements

Based on the results obtained for the white ABS (Figure 11a), the acetone treatment is very useful to extract the BFR, as the bromine has more affinity for the acetone than any of the other additives. Although the trends of Figure 11a are clear, it should be noted that the best mass balance was obtained for the titanium and implied that 77.22 ± 22.77 % of the initial amount of this element was accounted in the fractions obtained with the 4-step extraction process: supernatant, pellet, and residue (Figure 11b). Similarly, to iron (14.57 ± 4.31 %)), the bromine found was 16.90 ± 7.81 % of the initial amount of this element in the white ABS (Figure 11b). This might be related to the fact that the quantification of the additives with XRF has limitations and other methods should be used for a greater accuracy, such as the GC-MS for the bromine [10] and the ICP-OES for the trace metals [7]. Nevertheless, the XRF is very useful technique for initial characterization and sorting of the e-waste plastics based on the content of bromine. The acetone treatment might promote the volatilization of bromine; hence the extraction treatment needs to be robustly designed to prevent the gaseous emissions. Once the fraction of the white ABS has been solubilized, the repolymerization could be done with the antisolvent technique, by adding water to the acetone solution. Following this procedure, the bromide concentration found in reprecipitated ABS was found (2.9 mg/kg) to be much lower than the original concentration of this element in the raw white ABS sample (2939.3 mg/kg). This way of recycling the ABS minimized the volatilization of bromide, since this element remains in the acetone solution. In case the evaporation was allowed, the addition of virgin ABS (1.0 mg Br/kg) could minimize the loses of bromide and produce a semi-recycled material with 163.0 mg Br/kg. The acetone extraction of bromide is more convenient and effective that the use of more hazardous reagents, like the nitric acid (70 wt.%) that left the white ABS with a concentration of bromide of 305.0 mg/kg after 2 weeks of soaking with intermittent shaking (Table S1).

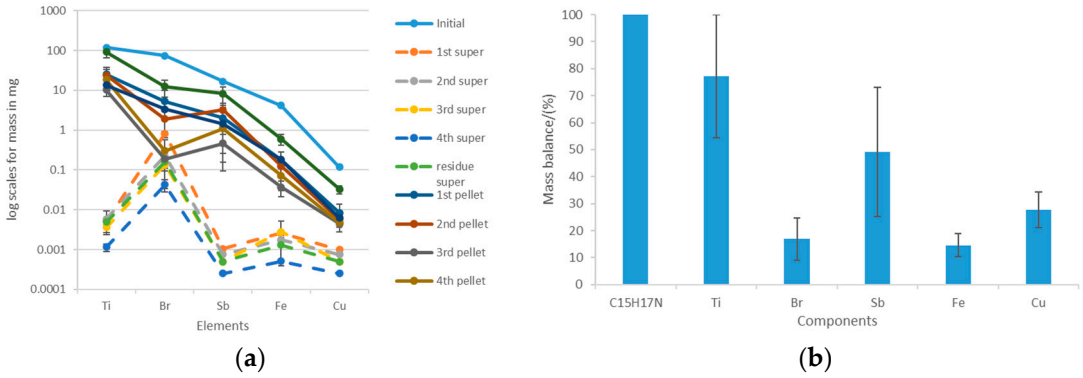

(**a**) (**b**)

Figure 11. Acetone-based extraction of the most abundant trace elements in the white ABS: (**a**) distribution of the elements among the supernatant and the pellet after each extraction step; (**b**) mass balances considering the initial amount of trace elements that were initially in the white ABS and the amounts that were found in the supernatant and the pellet.

The acetone treatment of the black ABS was not as effective as the extraction of bromide in the white ABS. As can be seen in Figure 12a, the elements that had greater affinity for the organic solvent were copper and nickel. As most of the bromine was found in the less soluble pellet fraction, the mass balance was met (Figure 12b) because the losses via volatilization were minimized. As with the white ABS, the 2-week treatment of the black ABS with nitric acid (70 wt.%) had poor capacity of removing the bromine but this soaking technique can be useful for other elements (Table S2): sulfur, neodymium, and nickel.

Preprints (www.preprints.org) | NOT PEER-REVIEWED | Posted: 30 March 2023 doi:10.20944/preprints202303.0516.v1

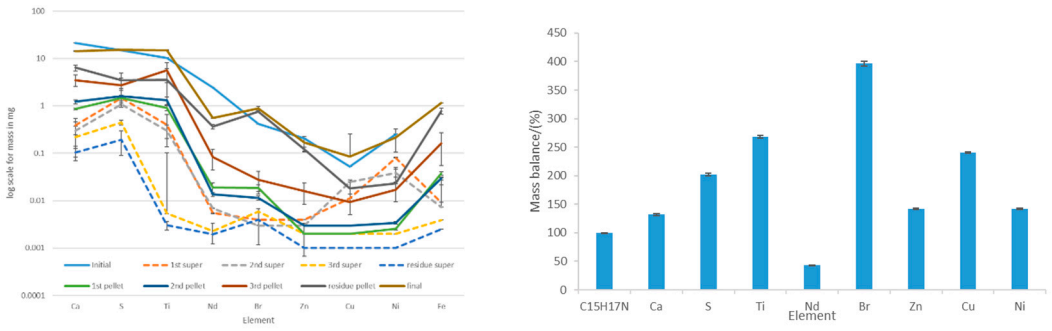

(**a**) (**b**)

Figure 12. Acetone-based extraction of the most abundant trace elements in the black ABS: (**a**) distribution of the elements among the supernatant and the pellet after each extraction step; (**b**) mass balances considering the initial amount of trace elements that were initially in the black ABS and the amounts that were found in the supernatant and the pellet.

The last combination possible of the bromide's affinity for the acetone and the recoverability of this element with the extraction method was observed with the ABS+PC (Figure 13). The processing of the e-waste plastic was characterized by the high affinity of the BFR for the acetone (Figure 13a) and also a high recoverability of this element (Figure 13 b). Unlike in the acetone-based treatment of the white ABS, where also the BFR had good affinity for the solvent but low bromide recoverability was found, the acetone-based treatment of the ABS+PC was supplemented with DCM after the 4th extraction. The results found was the recoverability of bromide increase significantly, although this effect might also be associated with the type of BFR compound that the ABS+PC contained. Overall, the concentration of bromide increased from 8.29 ± 0.16 mg/kg in the raw ABS+PC to 201.8 ± 85.70 mg/kg in the acetone-DCM-treated ABS+PC.

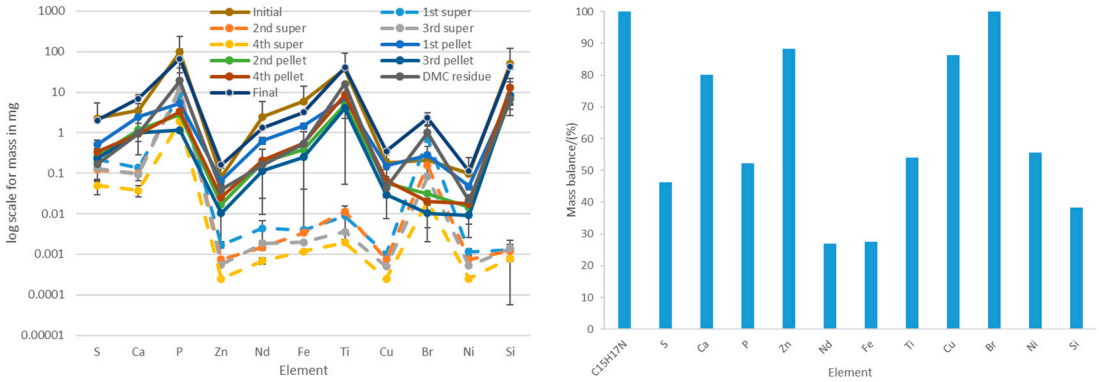

(**a**) (**b**)

Figure 13. Acetone-based extraction of the most abundant trace elements in the ABS+PC: (**a**) distribution of the elements among the supernatant and the pellet after each extraction step; (**b**) mass balances considering the initial amount of trace elements that were initially in the ABS+PC and the amounts that were found in the supernatant and the pellet.

3. Discussion

If the recycled e-waste plastic is intended for the packaging of foodstuff, the removal of the BFR might be required due to their persistence in the environment and the risks that these chemicals pose to public health [28]. According to the European Food Safety Authority [28], the plastics containing BFR, whether in use or waste, leach these chemicals to the environment and contaminate air, soil, and water; hence, these pollutants may enter the food chain. The consolidated version of the Waste Electrical and Electronic Equipment (WEEE) Directive of the EU, implementing the decision 2018/2193 prescribes proper treatment for the plastics containing BFR (Article 8 and Annex VII) [29].

 doi:10.20944/preprints202303.0516.v1

On the other hand, the lobby of the bromine industry BSEF [30] conducted an independent study to justify their products of BFR [31], being supported by Sofies international B-Corp certified sustainability consulting firm [32]. The problems of BFR are also known in the UK, although the charity Breast Cancer UK highlights that the organic flame retardants (including BFR, chlorinated flame retardants and organophosphorus flame retardants) are additive but they are not the most commonly used worldwide, unlike the aluminum hydroxide with 34 % of the market [33]. Additionally, the Drinking Water Inspectorate confirmed the leachability of the BFR and identified those with high potential for occurrence in water sources in the UK [34]. The UK Government [35] requires an special application to stablish the microfactories for the e-waste plastics. Particularly, the Department for Environment, Food & Rural Affairs of the UK still considers the use of the Best Available Treatment, Recovery and Recycling Techniques for the removal of plastic containing BFR [36]. Since the objective of removal is to ensure that BFR do not enter the material stream, unless the BFR are extracted it is not recommended the recycling of the plastics containing BFR [36]. The XRF can be implemented as a quick technique to identify bromide in e-waste plastics, enabling the separation of plastics containing BFR prior to recycling, energy recovery or disposal [37], otherwise the capacity of the current technologies for handling this materials will decrease [10]. In the case of the polybromodiphenyl ethers, which are a large group of 209 different type of BFR with similar chemical structure, the UK Government has provided specific guidance on how to respond to chemical incidents [38], as these compounds have particular potential to bioaccumulate in the environment [39], being the liver and thyroid likely toxicity target [40].

Given these limitations in the composition, a suitable application of the recycled filament was considering the manufacturing of hard drive caddies of different sizes. The different types of behavior of the e-waste plastics determine their suitability for different applications. The best combination to meet the mechanical specifications would be a blend of black ABS and PP with enough stiffness and flexibility. Since there are available in the market several grades of virgin polymers, the selection of the virgin material relied on the criteria of the melt-flow index (MFI) analysis. For example, for the ABS that is one of the polymers more widely used for 3D printing, the criteria was that the MFI should be around or below 10g/10min 210ºC/10kg (i.e. highly viscous materials). Materials with a MFI of 15g/10min 210ºC/10kg or greater are more suitable for recycling processes that include a molding-injection step rather than the melt-blend extrusion, due to the lower viscosity required [17]. The MFI technique was not used for the characterization of the e-waste plastics but the difficulties in the operation of the melt-blend extrusion step are an indicator of the suitability of the different materials for this type of valorization process. Figure 14a,b show several cross-sections of the clogging black ABS that was originated due to factors such as unmelted particles (Figure 14c,d), high moisture content that prevents the proper flow of the material, or even metal particles (Figure S45a) that accompanied the e-waste plastic and could only be unblocked with the Devoclean MidTemp purge (Figure S45b). Figure 14e,f show a filament with an unmelted core that went through the extrusion step due to the fusion of the outer layer, which upon cooling become a crust. As explained above, the valorization of the black ABS was done in 2 separate runs (Figure 4a,b) due to this undesired clogging. In Figure 7 all pictures were taken at the same magnification (x5) but the black ABS (Figure 7d) can be clearly seen thicker than the other filaments. This could be an explanation for the significant greater tensile strength that was found for this material (Figure 6a) and agrees with the greater viscosity of the black ABS. Figure S46 offers the microscope pictures of the thickest filament prepared with the clogging black ABS, before it was necessary to introduce the Devoclean MidTemp purge to continue with the operation of the equipment. It is noteworthy to mention that a homogenous composition of the filament is essential and the tensile strength will not increase otherwise. For this reason, despite the greater thickness of the clogging ABS, the mechanical strength was not enhanced (Figure 6a) since the filament was heterogeneous (Figure S47).

Preprints (www.preprints.org) | NOT PEER-REVIEWED | Posted: 30 March 2023 doi:10.20944/preprints202303.0516.v1

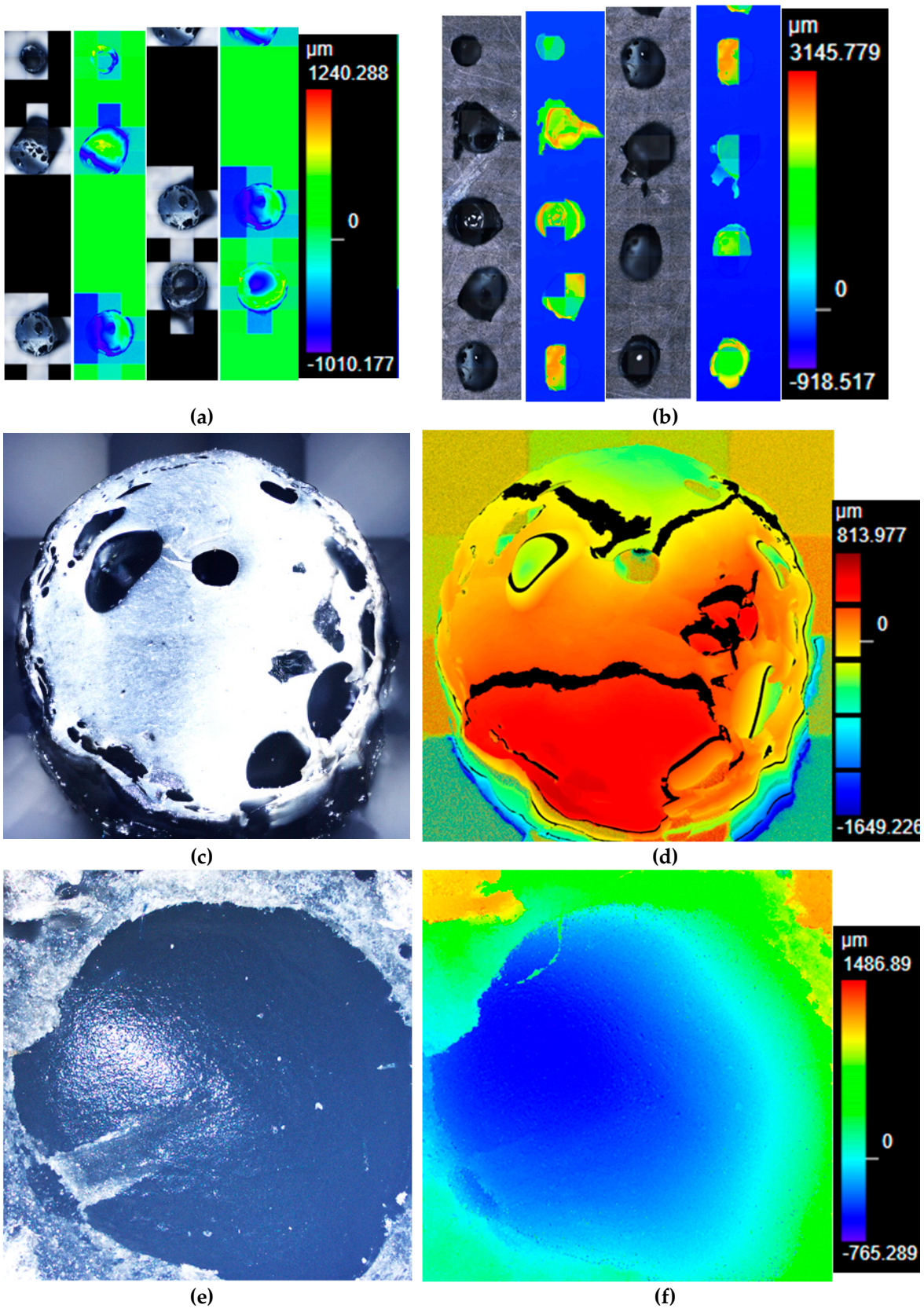

Figure 14. (**a**) laser microscope image (x10) of several cross-sectional areas of the filament of black ABS with unmelted particles; (**b**) laser microscope image (x10) several cross-sectional areas of the filament of black ABS with unmelted core; (**c**) laser microscope image (x20) of the cross-section of the filament of black ABS with unmelted particles; (**d**) laser scan (x20) of the cross-sectional area of the filament of black ABS with unmelted particles; (**f**) laser microscope image (x20) of the cross-section of

Preprints (www.preprints.org) | NOT PEER-REVIEWED | Posted: 30 March 2023 doi:10.20944/preprints202303.0516.v1

the filament of black ABS with unmelted core; and (**g**) laser scan (x20) of the cross-sectional area of the filament of black ABS with unmelted core.

Figure 15 depicts the layout of the microfactory for the manufacturing of hard drive caddies made of e-waste plastic. As part of the float-sink operation [7,41], the first tank full of water allows the mechanical separation of the PP (0.85 – 0.95 g/cm^3) from the ABS (1.04 – 1.06 g/cm^3) and the PC (1.20 – 1.22 g/cm^3) [7]. In order to be able to separate the ABS and the PC, it would be necessary to use a solvent, such as the DCM with a density of 1.33 g/mL and able to solubilize the PC [27]. Taking into account the problem of using DCM for Health & Safety and the environmental pollution, the manipulation of the density of the water with a brine of $CaCl_2$ could be more feasible. However, for complex mixtures of e-waste plastics the use of solvents (tertiary recycling) might be the only way to attain the complete separation for the polymer before the melt blend extrusion [4]. After this float-sink operation, the detection of additives and flame retardants will be possible with a portable handheld XRF equipment [42]. The results of the present investigation were considered to implement a short contact time between acetone and the ABS. This extraction step would give the best results because avoids excessive degradation of the matrix while still removing the BFR. The quick extraction of the trace elements of the ABS agrees with the techno-economic assessment of contact times lower than 90 minutes and avoid the degradation of the less soluble rubbery-phase of butadiene [19].

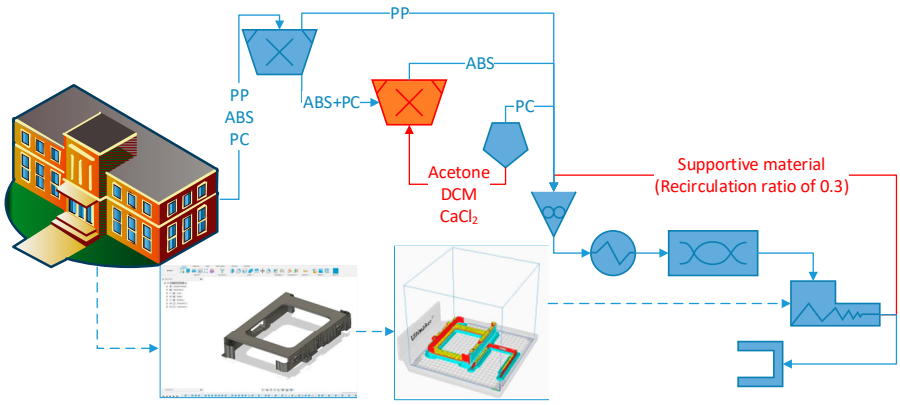

Figure 15. Design of a microfactory for the manufacturing of hard drive caddies with the recycled e-waste plastic polymers: ABS, PC, and PP.

In the next step of shredding, it is necessary to ensure a particle size below 2 mm for the heat subsequently devoted for the melting of the e-waste plastic to be as efficient as possible. Once the recycled 3D filament has been produced, a key decision to make is the type of component that will be replicated by additive manufacturing (Figure 48). The optimization of the use of the recycled material can be done with the software UltiMaker Cura [43], which informs how much supporting material will be necessary to print the component (Figure S48a). It is considered supported material all the recycled plastic that will be printed to maintain the parts of the component being replicated which deviates more than a 45º angle. In order to make this prediction, the only information that requires the software is the CAD file with the dimensions of the component that is going to be printed. For the hard drive caddies printed with ABS, 30 % of the recycled filament will be used as supportive material (Figure S48b). A recirculation loop has been included in Figure 15 to describe the mass flow of this supportive material that is removed from the printed component (Figure S48c) which needs to be reprocessed. Those components that require a large amount of supporting material when being printed might be more suitable for a microfactory including a molding injection step rather than the melt-blend extrusion. In case a visual element (e.g., screen frames of a laptop, mobile phone casings, etc.) would be printed, an additional downstream process step would need to be included in Figure 15 for the acetone smoothing. This last step of upgrading the printed piece before reaching the end-user is a very simple technique in which the acetone vapors are forced to interact with the borders of ABS, by means of a fan promoting the turbulence in the closed environment. Thereby, the 2 main

 doi:10.20944/preprints202303.0516.v1

variables that needed to be consider for the successful design of the recycling process (Figure S48d,e) were: the (chemical and mechanical) properties of the e-waste plastic and the structure of the component that is going to be replicated.

4. Materials and Methods

The most abundant e-waste plastics available in a recycling site in the UK were identified based on the indented RIC and the FTIR spectra. These were: ABS, PC, and PP. The difference in the composition of the matrix polymer (main component of the e-waste plastics) was characterized with the Cary 630 FTIR Spectrometer of Agilent Technologies, with ATR sampling module. Furthermore, the differences of the e-waste plastics in terms of the additives were characterized with XRF analysis: Shimadzu EDX8000 instrument equipped with a Rh sealed-source X-ray tube and a silicon strip detector. The samples were mounted on a Mylar film and were irradiated using a 5 mm in diameter collimator. Semi-quantitative concentrations were obtained using a Fundamental Parameter method.

The virgin materials to initiate the melt-blend extrusion process (HDPE, ABS, and PLA) were procured considering that these plastics should have an MFI below 10 (i.e. high viscosity). Before the melt-blend extrusion step, the reduction of the particle size to less than 5 mm was performed with the GP20 Shredder Hybrid of 3devo. The Precision 350 compounder of 3devo was used for processing the e-waste plastics following the protocols provided by the manufacturer of the equipment [15,16]. Devoclean MidTemp that initially contained the filament maker was purged with HDPE to ease the transition to the virgin ABS. In order to feed the virgin ABS, the settings used for the melt-blend extruder were: 4 heaters started at 240 ºC, screw speed at 5 rpm, and fan capacity at 50 %. Subsequently, the waste ABS was progressively introduced in the feedstock and once a stable operation was reached, the temperature of the heaters next to the feeding hoper was decreased down to 215 ºC [15]. Although ABS do not absorb a lot of moisture during storage, the drying was performed at 80°C for only 1 hour in the Airid Polymer Dryer of 3devo.

Similarly, the extrusion report prepared by 3devo was followed to assess the feasibility of recycling the waste PP. The virgin material that was used to ease the feeding of the PP was the PLA, using a bell-shaped setting of 170 – 175 ºC for the heaters of the extruder [16]. The preparation of the dumbbell-shaped specimen was done with the ZMorph 2.0 SX Multitool 3D Printer. The analysis of the filament thickness was performed with the optical sensor installed in the compounder and the software DevoVision. The characterization of the tensile strength of the filament was done with the equipment Instron 3345, which would be able to provide up to 5 kN of traction and compression forces. The Olympus LEXT OLS5000 SAF Optical 3D Measuring Laser Microscope was used for the characterization of the breakage of the recycled filaments. For the thermogravimetric analysis and the differential scanning calorimetry the NETZSCH STA 449 F3 Jupiter® was used. The acetone extraction of the white ABS was performed following a modified version of the protocol followed by Arostegui et al. [19]. The difference was that the samples were successively extracted up to 4 times, aiming the isolation of the most soluble fractions of the matrix (SAN copolymer) and additives (BFR) and minimizing the degradation of the rubbery dispersed fraction (butadiene). The subsequent extraction of the PC in the case of the ABS+PC was performed with DCM, similarly to Chandrasekaran et al. [27].

Supplementary Materials: The following supporting information can be downloaded at the website of this paper posted on Preprints.org, Figure S1: Laser microscope (x10) of the neck formation in the PP filament during the tensile test. Figure S2: Profile tensile force vs extension of the white ABS filament and the dumbbell shaped specimen prepared following the British Standard EN ISO 527-2:2012 (test conditions for molding and extrusion). Figure S3: Lose threads that can be seen in the filament made of 50 % virgin HDPE and 50 % virgin ABS upon rupture in the tensile testing. Figure S4: Tensile testing profiles for: (a) Commercial black ABS (8 replicates), (b) acetone smoothen white ABS (8 replicates), (c) virgin ABS (9 replicates), and (d) 10% white ABS + 90 % virgin ABS (10 replicates). Figure S5: Tensile testing profiles for: (a) 18 % white ABS + 82 % virgin ABS (10 replicates), (b) 35 % white ABS + 65 % virgin ABS (10 replicates), (c) 40 % white ABS + 60 % virgin ABS (15 replicates), and (d) 70 % white ABS + 30 % virgin ABS (10 replicates). Figure S6: Tensile testing profiles for: (a) 90 % white ABS + 10 % virgin ABS (10 replicates), (b) clogging ABS (10 replicates), (c) 50 % white ABS + 50 % black ABS (11

replicates), and (d) 50 % ABS+PC + 50 % black ABS (17 replicates). Figure S7: Tensile testing profiles for: (a) 50 % black ABS + 50 % HDPE (13 replicates), (b) 50 % virgin ABS + 50 % HDPE (10 replicates), (c) 50 % PP + 50 % PLA (21 replicates), and (d) 10 % PP + 90 % PLA (21 replicates). Figure S8: Thermogravimetric analysis (green line) and differencing scanning calorimetry (blue line) performed up to 600 ºC (red line) for the white ABS: (a) unprocessed waste and (b) the 1.75-mm filament obtained with the melt-blend extrusion. Figure S9: Thermogravimetric analysis (green line) and differencing scanning calorimetry (blue line) performed up to 600 ºC (red line) for the black ABS: (a) unprocessed waste and (b) the 1.75-mm filament obtained with the melt-blend extrusion. Figure S10: Thermogravimetric analysis (green line) and differencing scanning calorimetry (blue line) performed up to 600 ºC (red line) for the ABS+PC: (a) unprocessed waste and in (b) the 1.75-mm filament obtained with the melt-blend extrusion. Figure S11: Thermogravimetric analysis (green line) and differencing scanning calorimetry (blue line) performed up to 600 ºC (red line) for the PP: (a) unprocessed waste and in (b) the 1.75-mm filament obtained with the melt-blend extrusion. Figure S12: Thermogravimetric analysis (green line) and differencing scanning calorimetry (blue line) performed up to 600 ºC (red line) for the virgin ABS: (a) unprocessed pellet and in (b) the 1.75-mm filament obtained with the melt-blend extrusion. Figure S13: Thermogravimetric analysis (green line) and differencing scanning calorimetry (blue line) performed at the temperature informed by the red line for: (a) white ABS filament @ 800 ºC; (b) commercial black ABS filament @ 800 ºC; (c) commercial black ABS filament @ 600 ºC; (d) commercial green ABS @ 600 ºC. Figure S14: Thermogravimetric analysis (green line) and differencing scanning calorimetry (blue line) performed up to 600 ºC (red line) for: (a) fresh HDPE; (b) HDPE stored at room condition for a year; (c) MidTemp purge; (d) PLA filament. Figure S15: Comparisons of the FTIR spectra of the HDPE and the Devoclean MidTemp purge. Figure S16: Laser microscope images (x5) of the rupture of the filaments of Commercial black ABS filament in the tensile test. Figure S17: Laser microscope images (x5) of the failure of the filaments of 50 % white ABS 50 % Black ABS in the tensile test. Figure S18: Laser microscope images (x5) of the failure of the filaments of10 % white ABS 90 % virgin ABS in the tensile test. Figure S19: Laser microscope images (x5) of the rupture of the filaments of 18 % white ABS 88 % virgin ABS in the tensile test. Figure S20. Laser microscope images (x5) of the failure of the filaments of 25 % white ABS 75 % virgin ABS in the tensile test. Figure S21: Laser microscope images (x5) of the failure of the filaments of 35 % white ABS 65 % virgin ABS in the tensile test. Figure S22: Neck formation in the filaments of 35 % white ABS 65 % virgin ABS during the tensile test. Figure S23: Laser microscope images (x5) of the rupture of the filaments of 40 % white ABS 60 % virgin ABS in the tensile test. Figure S24: Neck formation in the filaments of 40 % white ABS 60 % virgin ABS in the tensile test. Figure S25: Laser microscope images (x5) of the rupture of the filaments of 70 % white ABS 30 % virgin ABS in the tensile test. Figure S26: Laser microscope images (x5) of the failure of the filaments of 70 % white ABS 30 % virgin ABS in the tensile test. Figure S27: Laser microscope images (x5) of the rupture of the filaments of 90 % white ABS 10 % virgin ABS in the tensile test. Figure S28: Laser microscope images (x5) of the failure of the filaments of virgin ABS in the tensile test. Figure S29: Laser microscope images (x5) of the rupture of the filaments of 50 % HDPE and 50 % Black ABS in the tensile test. Figure S30: Laser microscope images (x5) of the failure of the filaments of 50 % HDPE 50 % Black ABS in the tensile test. Figure S31: Laser microscope images (x5) of the rupture of the striations of the filament of ABS+PC. Figure S32: Laser microscope (x10) of the formation of 2 fibers in the PP filament during the tensile test. Figure S33: Laser microscope images (x5) of the neck formation in the filaments of 50 % PP + 50 % PLA during the tensile test. Figure S34: Laser microscope images (x5) of the failure of the filaments of 10 % PP 90 % PLA in the tensile test. Figure S35: Laser microscope images (x5) of the neck formation in the filaments of 10 % PP 90 % PLA during the tensile test. Figure S36: Laser microscope images (x5) of the rupture of the filaments of PLA. Figure S37: Laser microscope images (x5) of the failure of the filaments of PLA (with neck formation). Figure S38: TGA/DSC profiles of the fraction of white ABS isolated with the acetone extraction: (a) 1st supernatant, (b) 2nd supernatant, (c) 3rd supernatant, and (d) 4th supernatant. Figure S39: TGA/DSC profiles of the fraction of white ABS isolated with the acetone extraction: (a) 1st pellet, (b) 2nd pellet, (c) 3rd pellet, and (d) 4th pellet. Figure S40: TGA/DSC profiles of the fraction of the white ABS soaked for 2 weeks in nitric acid (70 wt.%) with intermittent shaking. Figure S41: TGA/DSC profiles of the fraction of black ABS isolated with the acetone extraction: (a) 1st supernatant, (b) 2nd supernatant, and (c) 3rd supernatant. Figure S42: TGA/DSC profiles of the fraction of black ABS isolated with the acetone extraction: (a) 1st pellet, (b) 2nd pellet, and (c) 3rd pellet. Figure S43: TGA/DSC profiles of the fraction of ABS+PC isolated with the acetone extraction: (a) 1st supernatant, (b) 2nd supernatant, (c) 3rd supernatant, and (d) 4th supernatant. Figure S44: TGA/DSC profiles of the fraction of ABS+PC isolated with the acetone extraction: (a) 1st pellet, (b) 2nd pellet, (c) 3rd pellet, and (d) 4th pellet. Table S1: Extraction of the white ABS with nitric acid (70 wt. %) conducted for 2 weeks with intermittent shaking. Table S2: Extraction of the black ABS with nitric acid (70 wt. %) conducted for 2 weeks with intermittent shaking. Figure S45: (a) Material that was found among the plastic e-waste. (b) Metal parts that remained inside the melt-blend extruder and they needed to be purged with Devoclean MidTemp (polyethylene). Figure S46: Laser microscope images (x5) of the rupture of the filaments of clogging ABS 100 % in the tensile test. Figure S47: Laser microscope images (x10) of

the failure of the filaments of Clogging ABS 100 % in the tensile test. Figure S48: (a) UltiMaker Cura visualization of the supportive material (blue color) that will be required to print the hard drive caddies with ABS. (b) Printed hard drive caddies with ABS. (c) Removal of the supportive material (30 % of the total ABS) from the hard drive caddies printed with ABS. (d) Proof that the small hard drive caddy fits for purpose. (e) Proof that the big hard drive caddy fits for purpose.

Author Contributions: Conceptualization, F.A.; methodology, A.M.A. and F.A.; software, A.M.A.; validation, A.M.A.; formal analysis, A.M.A.; investigation, A.M.A.; resources, F.A.; data curation, A.M.A.; writing—original draft preparation, A.M.A.; writing—review and editing, A.M.A. and F.A.; visualization, A.M.A.; supervision, F.A.; project administration, A.M.A. and F.A.; funding acquisition, A.M.A. and F.A. All authors have read and agreed to the published version of the manuscript.

Funding: This research was funded by the Accelerated Knowledge Transfer to Innovate (AKT2I) Pilot Scheme of the UKRI (Project Number 120 of Lancaster University).

Data Availability Statement: Restrictions apply to the availability of the data regarding the recycling company from where the e-waste plastics were sampled. Data of the stakeholders of this project is available upon request to the authors with the permission of third parties.

Acknowledgments: The authors would like to acknowledge the support received by Prof Allan Rennie, Samuel Walsh, Jessica Fisher, Tom Abram, Sebastian Smith, and Nicholas Renninson, Dr John Baum, and Dr Nathan Halcovitch.

Conflicts of Interest: The authors declare no conflict of interest. The funders had no role in the design of the study; in the collection, analyses, or interpretation of data; in the writing of the manuscript; or in the decision to publish the results.

Abbreviations

Acrylonitrile-butadiene-styrene (ABS); Brominated flame retardants (BFR); Dichloromethane (DCM); Differential scanning calorimetry (DSC); Fourier-transform infrared spectroscopy (FTIR); Melt-flow index (MFI); Polycarbonate (PC); Polylactic acid (PLA); Polypropylene (PP); Thermogravimetric analysis (TGA); poly(styrene-acrylonitrile) (SAN); Waste Electrical and Electronic Equipment (WEEE); X-ray fluorescence (XRF).

References

1. Jia, C.M.; Das, P.; Kim, I.; Yoon, Y.J.; Tay, C.Y.; Lee, J.M. Applications, treatments, and reuse of plastics from electrical and electronic equipment. *J. Ind. Eng. Chem.* **2022**, *110*, 84-99, doi:10.1016/j.jiec.2022.03.026.
2. Parajuly, K.; Kuehr, R.; Awasthi, A.K.; Fitzpatrick, C.; Lepawsky, J.; Smith, E.; Widmer, R.; Zeng, X. *Future e-waste scenarios*; 2019. Available online: https://ewastemonitor.info/e-waste-will-double-by-2050/ (accessed on 29 March 2023).
3. Wrap. *WEEE Collections Monitoring*; 2016. Available online: https://wrap.org.uk/resources/guide/weee-collection-guide (accessed on 29 March 2023).
4. Sahajwalla, V.; Gaikwad, V. The present and future of e-waste plastics recycling. *Current Opinion in Green and Sustainable Chemistry* **2018**, *13*, 102-107, doi:10.1016/j.cogsc.2018.06.006.
5. Das, A.; Debnath, B.; Chowdary, P.A.; Bhattacharyya, S. *Paradigm Shift in E-waste Management*; CRC Press: New York, 2022, doi: 10.1201/9781003095972
6. Baldé, C.P.; D'Angelo, E.; Luda, V.; Deubzer, O.; Kuehr, R. *The Global Transboundary E-waste Flows Monitor 2022*; Bonn, Germany, 2022. Available online: https://ewastemonitor.info/wp-content/uploads/2022/06/Global-TBM_webversion_june_2_pages.pdf (accessed on 29 March 2023).
7. Jia, C.; Das, P.; Kim, I.; Yoon, Y.J.; Tay, C.Y.; Lee, J.M. Applications, treatments, and reuse of plastics from electrical and electronic equipment. *Journal of Industrial and Engineering Chemistry* **2022**, *110*, 84-99, doi:10.1016/j.jiec.2022.03.026.
8. Martinho, G.; Pires, A.; Saraiva, L.; Ribeiro, R. Composition of plastics from waste electrical and electronic equipment (WEEE) by direct sampling. *Waste Management* **2012**, *32*, 1213-1217, doi:10.1016/j.wasman.2012.02.010.
9. Hunt, E.J.; Zhang, C.; Anzalone, N.; Pearce, J.M. Polymer recycling codes for distributed manufacturing with 3-D printers. *Resources, Conservation and Recycling* **2015**, *97*, 24-30, doi:10.1016/j.resconrec.2015.02.004.
10. Evangelopoulos, P.; Arato, S.; Persson, H.; Kantarelis, E.; Yang, W. Reduction of brominated flame retardants (BFRs) in plastics from waste electrical and electronic equipment (WEEE) by solvent extraction

and the influence on their thermal decomposition. *Waste Management* **2019**, *94*, 165-171, doi:10.1016/j.wasman.2018.06.018.
11. Zhan, F.; Zhang, H.; Cao, R.; Fan, Y.; Xu, P.; Chen, J. Release and Transformation of BTBPE During the Thermal Treatment of Flame Retardant ABS Plastics. *Environmental Science & Technology* **2019**, *53*, 185-193, doi:10.1021/acs.est.8b05483.
12. Environment Agency. *Polybrominated diphenyl ethers (PBDEs): sources, pathways and environmental data*; Bristol, 2019. Available online: https://consult.environment-agency.gov.uk/environment-and-business/challenges-and-choices/user_uploads/polybrominated-diphenyl-ethers-pressure-rbmp-2021.pdf (accessed on 29 March 2023).
13. He, Z.; Li, G.; Chen, J.; Huang, Y.; An, T.; Zhang, C. Pollution characteristics and health risk assessment of volatile organic compounds emitted from different plastic solid waste recycling workshops. *Environment International* **2015**, *77*, 85-94, doi:10.1016/j.envint.2015.01.004.
14. Woern, A.L.; McCaslin, J.R.; Pringle, A.M.; Pearce, J.M. RepRapable Recyclebot: Open source 3-D printable extruder for converting plastic to 3-D printing filament. *HardwareX* **2018**, *4*, e00026-e00026, doi:10.1016/j.ohx.2018.e00026.
15. 3devo B.V. *ABS extrusion report*; 2019. Available online: https://4595257.fs1.hubspotusercontent-na1.net/hubfs/4595257/Knowledge%20Base%20Import/ABS-Material-Report.pdf (accessed on 29 March 2023).
16. 3devo B.V. *PP extrusion report*. Available online: https://4595257.fs1.hubspotusercontent-na1.net/hubfs/4595257/Support%20Platform/downloadable%20PDF/Recycled-PP-Material-Report.pdf (accessed on 29 March 2023).
17. 3devo V.B. Material selection - Choosing the right polymer. Available online: https://support.3devo.com/guide-material-selection (accessed on 29 March 2023).
18. 3devo B.V. Research your own 3D printing materials. Innovate right from your desk. **2022**. Available online: https://www.3devo.com/ (accessed on 29 March 2023).
19. Arostegui, A.; Sarrionandia, M.; Aurrekoetxea, J.; Urrutibeascoa, I. Effect of dissolution-based recycling on the degradation and the mechanical properties of acrylonitrile–butadiene–styrene copolymer. *Polymer Degradation and Stability* **2006**, *91*, 2768-2774, doi:10.1016/j.polymdegradstab.2006.03.019.
20. Hirayama, D.; Nunnenkamp, L.A.; Braga, F.H.G.; Saron, C. Enhanced mechanical properties of recycled blends acrylonitrile–butadiene–styrene/high–impact polystyrene from waste electrical and electronic equipment using compatibilizers and virgin polymers. *Journal of Applied Polymer Science* **2022**, *139*, 1-11, doi:10.1002/app.51873.
21. Ramesh, V.; Biswal, M.; Mohanty, S.; Nayak, S.K. Recycling of engineering plastics from waste electrical and electronic equipments: Influence of virgin polycarbonate and impact modifier on the final performance of blends. *Waste Management and Research* **2014**, *32*, 379-388, doi:10.1177/0734242X14528404.
22. 3devo B.V. Filament Maker Quality Check. Available online: https://support.3devo.com/filament-maker-quality-check (accessed on 29 March 2023).
23. British Standard Institution. BS EN ISO 527-2:2012. **2012**. Available online: https://landingpage.bsigroup.com/LandingPage/Standard?UPI=000000000030216860 (accessed on 29 March 2023).
24. Zhang, J.; Hirschberg, V.; Rodrigue, D. Blending Recycled High-Density Polyethylene HDPE (rHDPE) with Virgin (vHDPE) as an Effective Approach to Improve the Mechanical Properties. *Recycling* **2022**, *8*, 2-2, doi:10.3390/recycling8010002.
25. Yahiaoui, M.; Denape, J.; Paris, J.Y.; Ural, A.G.; Alcalá, N.; Martínez, F.J. Wear dynamics of a TPU/steel contact under reciprocal sliding. *Wear* **2014**, *315*, 103-114, doi:10.1016/j.wear.2014.04.005.
26. Kim, J.K.; Kang, C.K. Basic Studies on Recycling of ABS Resin. *Polymer-Plastics Technology and Engineering* **1995**, *34*, 875-890, doi:10.1080/03602559508012182.
27. Chandrasekaran, S.R.; Avasarala, S.; Murali, D.; Rajagopalan, N.; Sharma, B.K. Materials and Energy Recovery from E-Waste Plastics. *ACS Sustainable Chemistry and Engineering* **2018**, *6*, 4594-4602, doi:10.1021/acssuschemeng.7b03282.
28. EFSA. Brominated Flame Retardants. Available online: https://www.efsa.europa.eu/en/topics/topic/brominated-flame-retardants#:~:text=Other%20brominated%20flame%20retardants.%20These%20classes%20have%20been,the%20risks%20these%20chemicals%20pose%20to%20public%20health. (accessed on 29 March 2023).
29. Directive 2012/19/EU of the European Parliament and of the Council of 4 July 2012 on waste electrical and electronic equipment (WEEE). **2019**. Available online: https://eur-lex.europa.eu/legal-content/EN/TXT/PDF/?uri=CELEX:32012L0019&from=EN (accessed on 29 March 2023).
30. BSEF. About BSEF. Available online: https://www.bsef.com/about-us/about-bsef/ (accessed on 29 March 2023).
31. Sofies. Study on the Impacts of Brominated Flame Retardants on the Recycling of WEEE plastics in Europe. **2020**, 25-25. Available online: https://www.bsef.com/wp-content/uploads/2020/11/Study-on-the-impact-of-

Brominated-Flame-Retardants-BFRs-on-WEEE-plastics-recycling-by-Sofies-Nov-2020.pdf (accessed on 29 March 2023).
32. BSEF. Brominated flame retardants are not hindering the recycling of weee plastics says new study. **2020**. Available online: https://www.bsef.com/news/sofiesreport/ (accessed on 29 March 2023).
33. Breast Cancer, U.K. *Flame retardants*; 2017. Available online: https://www.breastcanceruk.org.uk/app/uploads/2019/08/Background_Briefing_Flame_retardants_21.9.17_IS_nw.pdf (accessed on 29 March 2023).
34. Vince, S. *Brominated flame retardants - risks to UK drinking water sources*; 2009. Available online: https://dwi-content.s3.eu-west-2.amazonaws.com/wp-content/uploads/2020/10/27110953/DWI70_2_219.pdf (accessed on 29 March 2023).
35. Government, U.K. Waste electrical and electronic equipment (WEEE): reuse and treatment. **2019**. Available online: https://www.gov.uk/guidance/waste-electrical-and-electronic-equipment-weee-reuse-and-treat (accessed on 29 March 2023).
36. DEFRA. *Guidance on Best Available Treatment Recovery and Recycling Techniques (BATRRT) and treatment of Waste Electrical and Electronic Equipment (WEEE)*; 2006. Available online: https://webarchive.nationalarchives.gov.uk/ukgwa/20130402151656/http://archive.defra.gov.uk/environment/waste/producer/electrical/documents/weee-batrrt-guidance.pdf (accessed on 29 March 2023).
37. WRAP. *Develop a process to separate brominated flame retardants from WEEE polymers*; 1844051471; 2006. Available online: https://www.researchgate.net/publication/236838704_WRAP_Project_PLA-037_develop_a_process_to_separate_brominated_flame_retardants_from_WEEE_polymers_Interim_Report_2_The_Waste_and_Resources_Action_Programme_Banbury_UK (accessed on 29 March 2023).
38. UK Government. Brominated flame retardants: incident management and toxicology. **2018**. Available online: https://www.gov.uk/government/publications/brominated-flame-retardants-properties-incident-management-and-toxicology (accessed on 29 March 2023).
39. Birnbaum, L.S.; Staskal, D.F. Brominated flame retardants: cause for concern? *Environmental Health Perspectives* **2004**, *112*, 9-17, doi:10.1289/ehp.6559.
40. Toxicology Department Public Health England. *Polybromodiphenyl ethers (Decabromodiphenyl ether): General Information*; 2009. Available online: https://assets.publishing.service.gov.uk/government/uploads/system/uploads/attachment_data/file/341393/Deca_BDE_General_Information_phe_v1.pdf (accessed on 29 March 2023).
41. Poulakis, J.G.; Papaspyrides, C.D. Recycling of polypropylene by the dissolution/reprecipitation technique: I. A model study. *Resources, Conservation and Recycling* **1997**, *20*, 31-41, doi:10.1016/S0921-3449(97)01196-8.
42. Dimitrakakis, E.; Janz, A.; Bilitewski, B.; Gidarakos, E. Determination of heavy metals and halogens in plastics from electric and electronic waste. *Waste Management* **2009**, *29*, 2700-2706, doi:10.1016/j.wasman.2009.05.020.
43. UltiMaker B.V.. UltiMaker Cura. Available online: https://ultimaker.com/software/ultimaker-cura (accessed on 29 March 2023).